Environment International 129 (2019) 438–450

Contents lists available at ScienceDirect

Environment International

journal homepage: www.elsevier.com/locate/envint

Changes in spatio-temporal patterns of urban forest and its above-ground carbon storage: Implication for urban CO_2 emissions mitigation under China's rapid urban expansion and greening

Zhibin Ren[a], Haifeng Zheng[a,*], Xingyuan He[a,*], Dan Zhang[a,b], Guoqiang Shen[a], Chang Zhai[a]

[a] Key Laboratory of Wetland Ecology and Environment, Northeast Institute of Geography and Agroecology, Chinese Academy of Sciences, 4888 Shengbei Road, Changchun, Jilin Province, 130102, China

[b] Horticultural College, Changchun University, 6543 Weixing Road, Changchun, Jilin Province, 130022, China

ARTICLE INFO

Handling Editor: Yong-Guan Zhu

Keywords:
Urban forest (UF)
Urbanization
Carbon storage
Urban greening

ABSTRACT

Background: Understanding spatio-temporal dynamics of UF and its above-ground carbon storage (CS) is important for mitigating urban CO_2 emissions under China's rapid urban expansion and greening.

Methods: In our study, vegetation index (VI) data obtained from TM image and CS derived from field-based surveys were amalgamated to develop a regression model to predict spatio-temporal patterns of CS. VI correction model was established by normalizing previous imagery (1984, 1995, and 2005) to 2014 image data.

Results: NDVI is better than other VIs for predicting urban forest CS. Both UF area and its CS increased gradually from 1984 to 2014, especially in outer rings of the city. CS showed a definite decreasing trend from outer rings to downtown. Due to urban greening policies, landscape patches of UF or CS recently became larger and more aggregated. The CS by UF class distribution was skewed toward low values in all the years, but the skew gradually decreased over time. It was estimated that the average annual increase of CS by UF could offset 3.9% of the average annual increase in urban carbon emissions.

Conclusions: Our study proposes that spatio-temporal changes in UF patterns dramatically affected the amount of CS and carbon capture. The increase in UF coverage and quality would mitigate more urban carbon emissions, especially in outer rings.

1. Introduction

In the past six decades, China has witnessed rapid urbanization (Wu et al., 2012; Wang et al., 2019). Chinese cities produce more and more CO_2 because of the rapid urban development. Recently, China government has set up many CO_2 mitigation strategies in cities, such as an increasing emphasis on urban forest (UF) construction (Yang et al., 2014; Zhao et al., 2013). It is widely accepted that UF can act as an important sink for urban CO_2 emission in cities by transforming CO_2 into urban plant biomass (Nowak and Crane, 2002; Lucy et al., 2010).

An empirical study showed urban forest carbon sequestration in United States can account for about 14% of the entire amount of the nation's forests (Heath et al., 2011; Nowak et al., 2013). In recent years, UF in China has been greatly developed (Zhou and Wang, 2011; Wang, 2016; Pei et al., 2018). For example, Urban Forest City Programs were proposed from 2004 and many governmental regulations relating to urban greening have been introduced (Jiang and Zhang, 2010; Wang, 2016). A designation of “forest city” has been established to recognize cities that achieve the coverage of urban green spaces > 35% and per capita green space availability of > 9 m^2. As of 2016, there are 118 forest cities in China and over 80 cities are pursuing the title. This is a good opportunity for UF construction to offer great potential for CO_2 sequestration in these Chinese cities. However, the ecological consequences of those National urban forest planting policies are still not clear. In addition, these kinds of ecological services are often largely underestimated, and the potential of UF themselves to mitigate CO_2 emission and climate change are far from being understood (Gaston et al., 2013). Therefore, the accurate and timely estimation of UF carbon storage (CS) is essential for urban managers to design systems to improve urban CO_2 emissions mitigation.

It is labor intensive and costly to obtain spatial-temporal CS data in large scale metropolitan regions by conventional plot-based sampling methods (Liu and Li, 2012; Zhang et al., 2015; Escobedo et al., 2010; Nero et al., 2018). The development of remote sensing technology

* Corresponding authors.
E-mail addresses: zhenghaifeng@iga.ac.cn (H. Zheng), hexingyuan@iga.ac.cn (X. He).

https://doi.org/10.1016/j.envint.2019.05.010
Received 27 January 2019; Received in revised form 5 May 2019; Accepted 5 May 2019
Available online 30 May 2019

provides an opportunity to estimate the patterns of CS by UF from satellite imagery (Frolking et al., 2009). Many studies showed the remote sensing data could be combined with field survey data to quantify the carbon pool of urban vegetation (Raciti et al., 2014; Lee et al., 2016; Sun et al., 2019). Urban vegetation CS was calculated in many cities across the world, such as Sacramento, CA (2.7×10^6 t) (McPherson et al., 2013), Boston, MA (355 Gg) (Raciti et al., 2014) in USA; cities in China like Beijing (956.3 Gg) (Sun et al., 2019), Hangzhou (11.74 Tg) (Zhao et al., 2010); Leipzig, Germany(316,000 Mg) (Strohbach and Haase, 2011); Kumasi, Ghana(1.2×10^6 t) (Nero et al., 2018),etc. However, there are relatively few studies showing the spatio-temporal change of UF carbon storage caused by the rapid urbanization. The comprehensive effects of rapid urban expansion and urban greening on spatial patterns of CS by UF with a long time span are still not well understood. The higher resolution remote sensing data appearing in recent years such as QiuckBird and SPOT can be used for forest carbon extraction with high accuracy (Rao et al., 2013; Lv et al., 2016; Narine et al., 2019). However, this kind of data usually had a short time span and hardly obtained before 2000. In addition, these data are often more expensive. While Landsat Thematic Mapper (TM) imagery is easily accessed and is widely used since 1972 all over the world to estimate forest structural and functional attributes. Many researchers have developed techniques for the assessment of forest structures and functions using spectral vegetation indices (VIs) from TM remote sensing imagery (e.g., Roy et al., 1991; Cohen et al., 1995; Kayitakire et al., 2006). Previous studies have showed that the some VIs obtained from TM or ETM+ remote sensing data are significantly correlated with ground measured natural forest structures as canopy cover, stem density, diameter, tree height, etc. (Ingram et al., 2005; Simone et al., 2005; Ji et al., 2012). Researchers have achieved some degree of success in estimating forest biomass or carbon storage from TM data in natural areas worldwide. However, the statistical relationships between forest biomass or CS and VIs vary with the characteristics of ecosystem (Lu et al., 2004). Compared with natural forests, UF usually is heterogeneous, fragmented, scattered, and surrounded by many impervious surfaces. There are some studies in the literature estimating spatial patterns of CS by UF with plot-based sampling methods (Nowak and Greenfield, 2012; Liu and Li, 2012). However, whether TM or ETM + imagery can still be used and which vegetation index extracted from TM imagery can be practically used for estimating spatio-temporal UF biomass or CS is still unknown.

Changchun is a typical industrial city with recent rapid urbanization in temperate region of northeastern China. There are little data showing the contribution of changes in spatio-temporal patterns of urban forest and its carbon storage to offsetting urban CO_2 emissions under rapid urbanization in such kind of cities, China. Field observations were conducted in 2013/2014 and TM images data were acquired for four different years (1984, 1995, 2005, and 2014) for the city which provided the base data for this study. The objectives of this study are to: (1) examine the practicability of TM remote sensing in estimating spatio-temporal changes of UF and its CS, (2) develop model for estimating CS by coupling field measurements with TM remotely sensed data, (3) explore the dynamic patterns of UF and its CS from 1984 to 2014 under China's rapid urban expansion and greening, (4) investigate the contribution of urban forest CS to offsetting urban CO_2 emissions and the implications of UF for CO_2 emissions mitigation in China.

2. Methods

2.1. Study area

This study was conducted in the city of Changchun (125°09′-125°48′E, 43°46′-43°58′N) (Fig. 1), China, which is an important social-economic center of northeastern China. The city's down town was

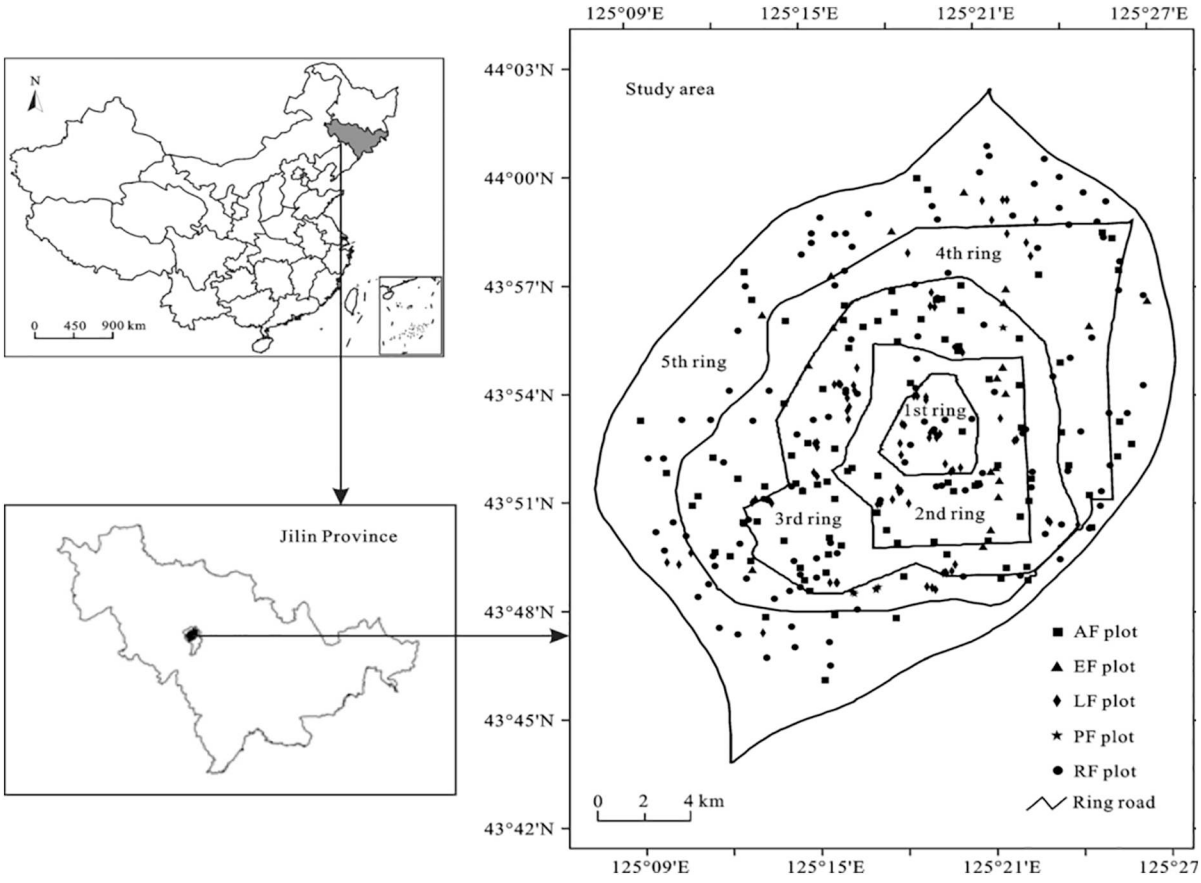

Fig. 1. The study area located within the fifth-ring road in the city of Changchun, China.

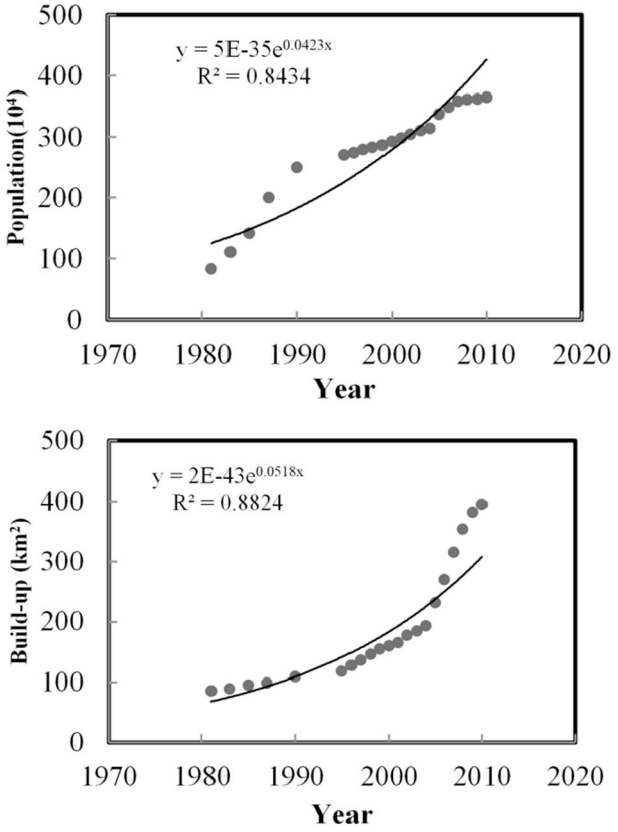

Fig. 2. Urbanization in Changchun city from 1980 to 2014.

surrounded by several concentric ring roads (from 1st to 5th ring). The average total yearly rainfall is 567 mm and the average temperatures in winter and summer are −14 °C and 24 °C, respectively. Changchun is called a "Forest city" with vegetation coverage of 45% in 2016 (SFA, 2018). Urban tree species are most abundant with 43 families, 86 genera, and 211 species (Zhang et al., 2015). Changchun has experienced an accelerated process of urbanization during the last 30 years (1984–2014) (Fig. 2), Urban build-up area was 89 km^2 in 1984 and reached to 430 km^2 in 2014, an increase of 10 km^2 for each year. Urban population increased from 1.1 million in 1984 to 4.1 million in 2014, an increase of 90,000 for each year. In addition, Changchun is a typical important industrial city in China with the highest energy consumption and more and more CO_2 was produced from this kind of Chinese cities (Zhang et al., 2015). Therefore, this city is an ideal area for investigating the spatio-temporal patterns of UF and its CS.

2.2. Image data processing and UF extraction

Four sets of TM images were collected on September 14, 1984, September 29, 1995, September 08, 2005 and October 03, 2014, with a cloud cover < 5%. The images have a ground resolution of 30 m per pixel for most bands. The atmospheric correction for the TM images was first undertaken with the method of FLAASH Atmospheric Correction in ENVI 4.6 (Exelis Visual Information Solutions, Boulder, CO, USA). After atmospheric correction, the pop curve of vegetation is more closer to the real vegetation pop curve. The TM raw digital numbers (DN) were then converted into surface radiance values following the procedures provided by Chander and Markham (2003). Finally, the TM images were geo-referenced to WGS-84 Universe Transverse Mercador (UTM) coordinate system with a root mean square error (RMSE) of < 0.5 pixel (225 m^2) by using 33 ground control points taken from topographic maps. Based on the four scenes of TM images, the five VIs were then

Table 1
The used Landsat-derived vegetation index and their relationship with urban CS.

Index	Equation	Pearson's correlation coefficients
NDVI	$NDVI = (b_4 - b_3) / (b_4 + b_3)$	0.738[b]
SR	$SR = (b_4 / b_3)$	0.519[a]
GNDVI	$NDII = (b_4 - b_2) / (b_4 + b_2)$	0.564[a]
NDMI	$NDMI = (b_4 - b_5) / (b_4 + b_5)$	0.464[a]
NLI	$NLI = (b_5^2 - b_7) / (b_5^2 + b_7)$	0.209

Where b_2, b_3, b_4, b_5 and b_7 are surface reflectance values in Landsat TM bands 2, 3, 4, 5 and 7, respectively Citation.
[a] Correlation is significant at α = 0.05 level (two-tailed).
[b] Correlation is significant at α = 0.01 level (two-tailed).

Table 2
Image normalization coefficients and corresponding model R-squared for each subject image obtained by linear regression.

	1984	1995	2005
a	0.712	0.745	0.876
b	−0.154	−0.103	−0.095
R^2	0.725	0.712	0.842

calculated from TM images (Table 1) in ENVI 4.6. UF can be defined as urban green space with area larger than 0.5 ha, with trees as the main vegetation, considerably influencing surrounding environment, and providing effective ecological and landscape values (Liu et al., 2003). Generally, urban green spaces in China were covered by trees, shrubs and grass together, especially for the larger patches. Therefore, only those green space patches with area larger than 0.5 ha were extracted as UF in our study. Based on four scenes of TM images, a three-level hierarchical object-based approach was used for UF extraction in eCogntion9.0 software (Zhou and Troy, 2009). This technique used to analyze digital imagery, is based on information from a set of similar pixels called objects or image objects. The TM images were first segmented into objects by an object-based approach and then assigned to an UF class. It is superior to traditional pixel-based classification (Gao and Mas, 2008). For example, the "salt-and-pepper" effect frequently found in pixel-based classification can be largely avoided when an object-based approach is used for land cover classification. Sixty random points for the four UF maps were created separately using a stratified random sampling method for the accuracy assessment. The historical high spatial resolution images in Google Earth™ Timelapse were used as reference data for the accuracy assessment. The acquisition year for Google Earth images was matching the year for acquiring the multitemporal TM images. The overall accuracies of UF extraction for 1984, 1995, 2005 and 2014 were 89.24%, 90.43%, 91.58% and 93.12%, respectively.

2.3. Landscape metrics analysis

It is very important to select appropriate metrics for analysis of urban forest landscape patterns. The two main criteria were followed for the selection of landscape patterns metrics (Schindler et al., 2015; Kwok et al., 2016): 1). Metrics examine the various aspects of landscape pattern characteristics such as size, edge, shape, fragmentation, and connectivity; 2). Metrics should not be highly redundant. These selected metrics include Number of Patches (NP), Patch Density (PD), Patch Area Mean (PAM), Edge Density (ED), Largest Patch Index (LPI), Landscape Shape Index (LSI), Aggregation Index (AI) and Patch Cohesion Index (COHESION). NP equals the number of patches of the UF; PD equals the number of UF patches, divided by total UF area; PAM equals

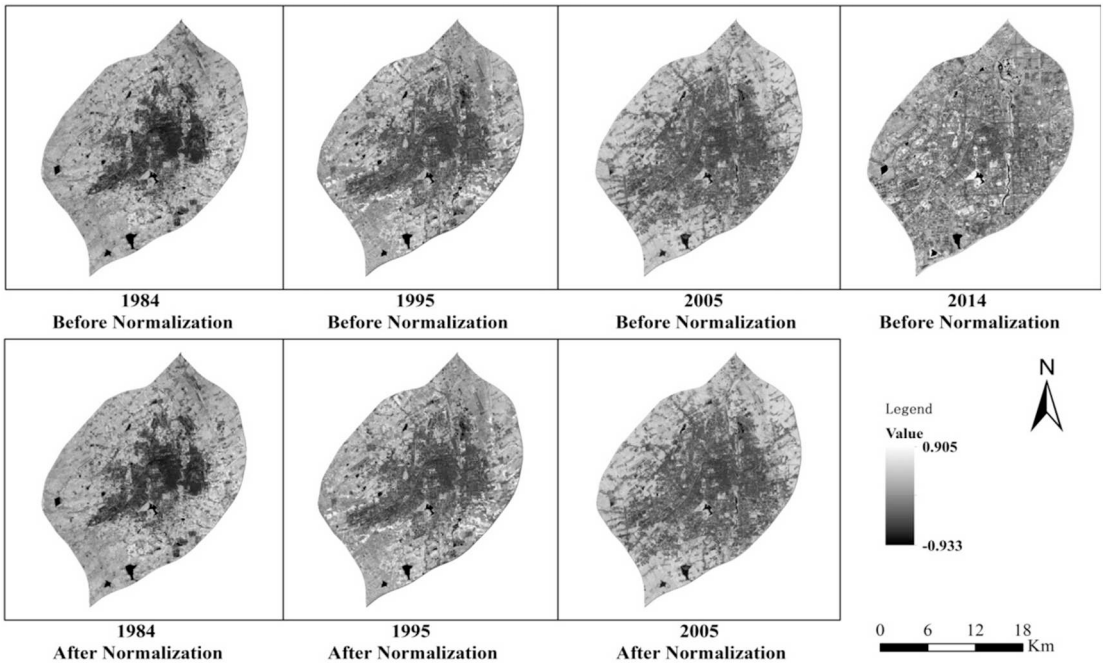

Fig. 3. The NDVI images before and after normalization.

the sum, across all UF patches, divided by the total number of patches; ED equals the sum of the lengths of all edge segments involving the UF patch, divided by the total UF area; LPI equals the percentage of the landscape comprised by the largest patch; LSI equals 0.25 (adjustment for raster format) times the sum of the entire UF boundary and all edge segments within the landscape boundary, including some or all of those bordering background, divided by the square root of the total UF area; AI equals the number of like adjacencies involving the corresponding class, divided by the maximum possible number of like adjacencies, which is achieved when the UF patch is maximally clumped into a single, compact patch; COHESION equals 1 minus the sum of patch perimeter divided by the sum of patch perimeter times the square root of patch area for patches, divided by 1 minus 1 divided by the square root of the total number of cells in the landscape, multiplied by 100 to convert to a percentage. We calculated landscape metrics for UF at the landscape level using the computer program FRAGSTATS (McGarigal et al., 2012, The University of Massachusetts, Amherst, MA. USA). FRAGSTATS is a computer software program designed to compute a wide variety of landscape metrics for categorical map patterns, which was released in 1995.

2.4. Sampling design and CS calculation

A total of 159 UF plots throughout the study area were established by the stratified random sampling methods used in the Urban Forest Effects (UFORE) Model (Nowak et al., 2003). The UFORE computer model was developed to help managers and researchers quantify UF structure and functions by U.S. Forest Service in 2000. Field measurements were conducted during July and August 2013 and 2014 (Fig. 4).The sampling plots were randomly selected to ensure they were representative of the major land cover types such as residential, road, park and commercial areas in Changchun. A sampling plot was required to be located in a relatively homogenous patch > 0.5 ha. Each of the 159 sampling plots was defined as 30 × 30 m^2 (0.09 ha) to conform to a TM pixel size. The coordinates of each sampling plot were recorded with global positioning system (MG838GPS) with the accuracy better than 1 m. At each sampling plot, UF structural attributes including tree species, UF types, stem density, diameter at breast height (DBH), tree height (H), and crown closure were measured and recorded.

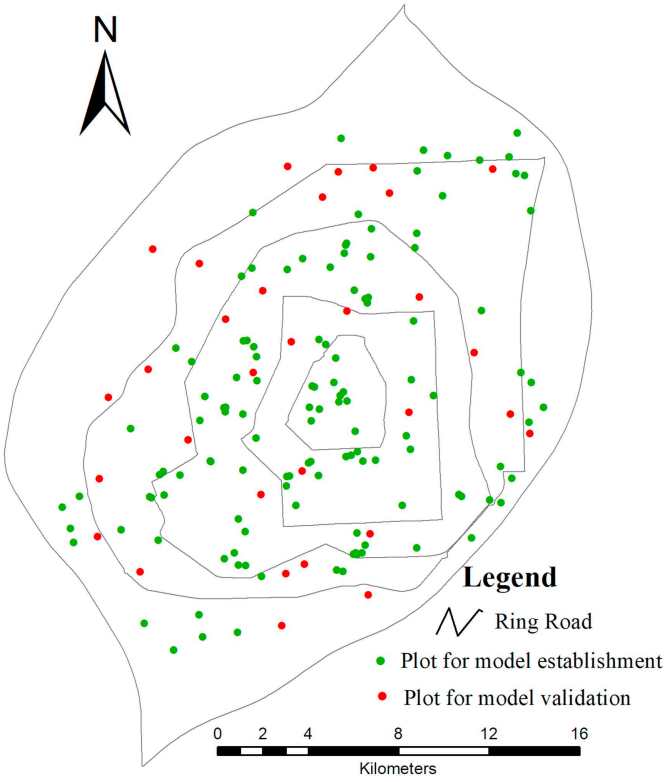

Fig. 4. Map of 159 sampling plots in the City of Changchun, Jilin Province, China.

The above-ground dry biomass of each surveyed tree was first estimated using biomass allometric growth equations obtained from the literature (Supplementary Table 1) (Wang, 2006; Wu et al., 2012; Liu and Li, 2012). Either the DBH alone, or a combination of the DBH and

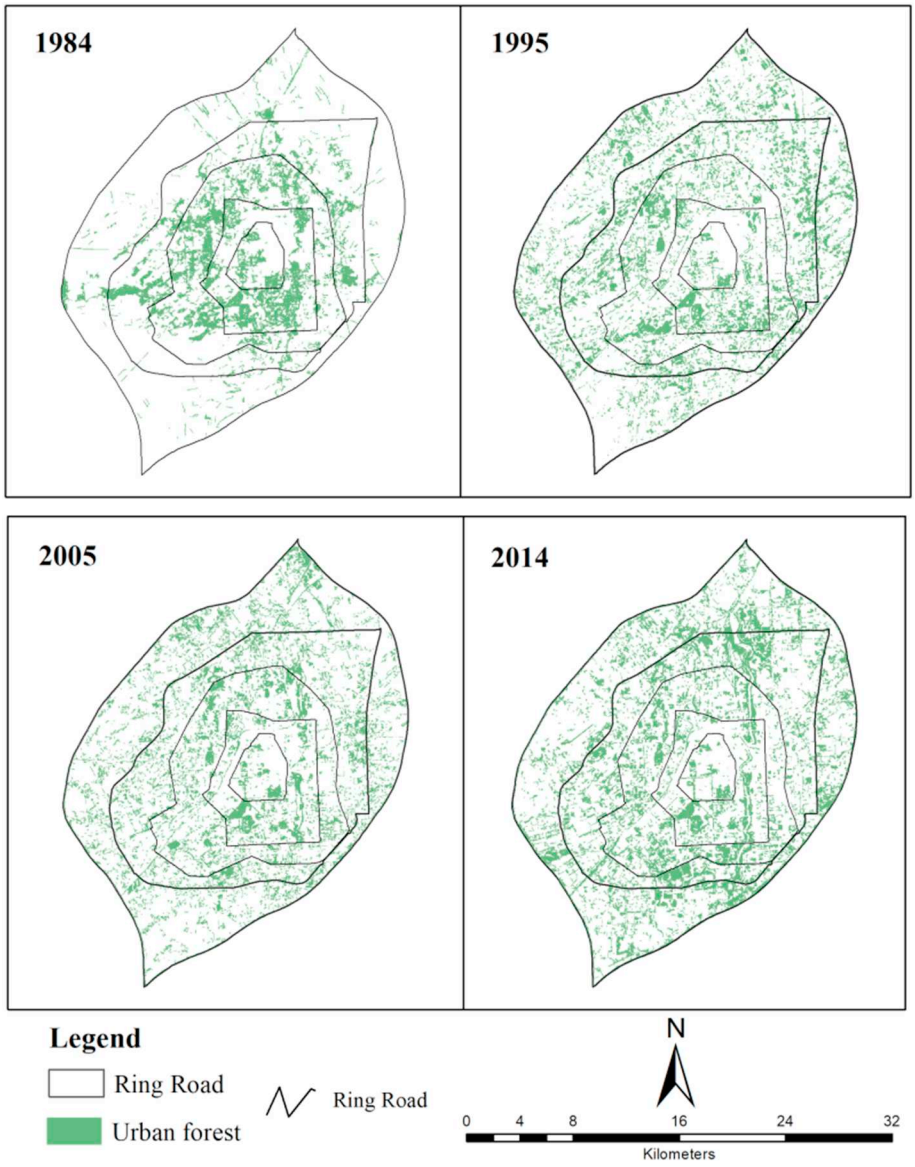

Fig. 5. Spatio-temporal patterns of UF in Changchun during 1984–2014.

tree height (H) were used to calculate the individual tree biomass. The equations for geographic areas which were closer to our study area were selected in our study for biomass calculation (Liu and Li, 2012). When we could not find species-specific allometric equation, equations for species affiliated to the same genus or family were used. When no equations were found for a genus or a family, a generalized equation from McPherson et al. (2013) and Wang (2006) was used. Because of severe pruning and maintenance, urban trees tend to have less above-ground biomass than that estimated by equations derived for natural forests (Nowak, 1994). Therefore, the estimated biomass was calculated by multiplying the calculated biomass by 0.8 (Nowak, 1994). The dry biomass for each plot was then converted to carbon by multiplying by 0.5 (Nowak, 1994; Nowak and Crane, 2002).

VI values were extracted from the normalized TM images in ArcGIS 10.3 software (ESRI, Redlands, CA, USA) and tagged with the latitude and longitude coordinates for each sampling plot for subsequent statistical analyses.

2.5. Spatio-temporal estimation of CS with TM images

First, we conducted the correlation analyses between urban forest CS collected from 129 plots and corresponding VIs values extracted from the 2014 VIs map. Next, the best VI for predicting the urban forest CS were selected in our study. Finally, a quantitative regression model was established based on CS data collected from the 129 plots and the corresponding best VI data extracted from the 2014 TM image. The extracted plot-based VI data were used as the independent variable and CS was used as a dependent variable. Coefficient of determination (R^2) for regression analysis was used to assess the performance of the model. To evaluate the reliability and accuracy of the established model, measured CS data for 30 plots (Fig. 4) were used for validation. R^2 and RMSE were used to test the goodness-of-fit of the prediction model at plots. All statistical analyses were carried out with standard statistical software, SPSS (Version 19.0, Armonk, NY, USA: IBM Corp.).

In order to conduct spatiotemporal analyses of UF carbon storage

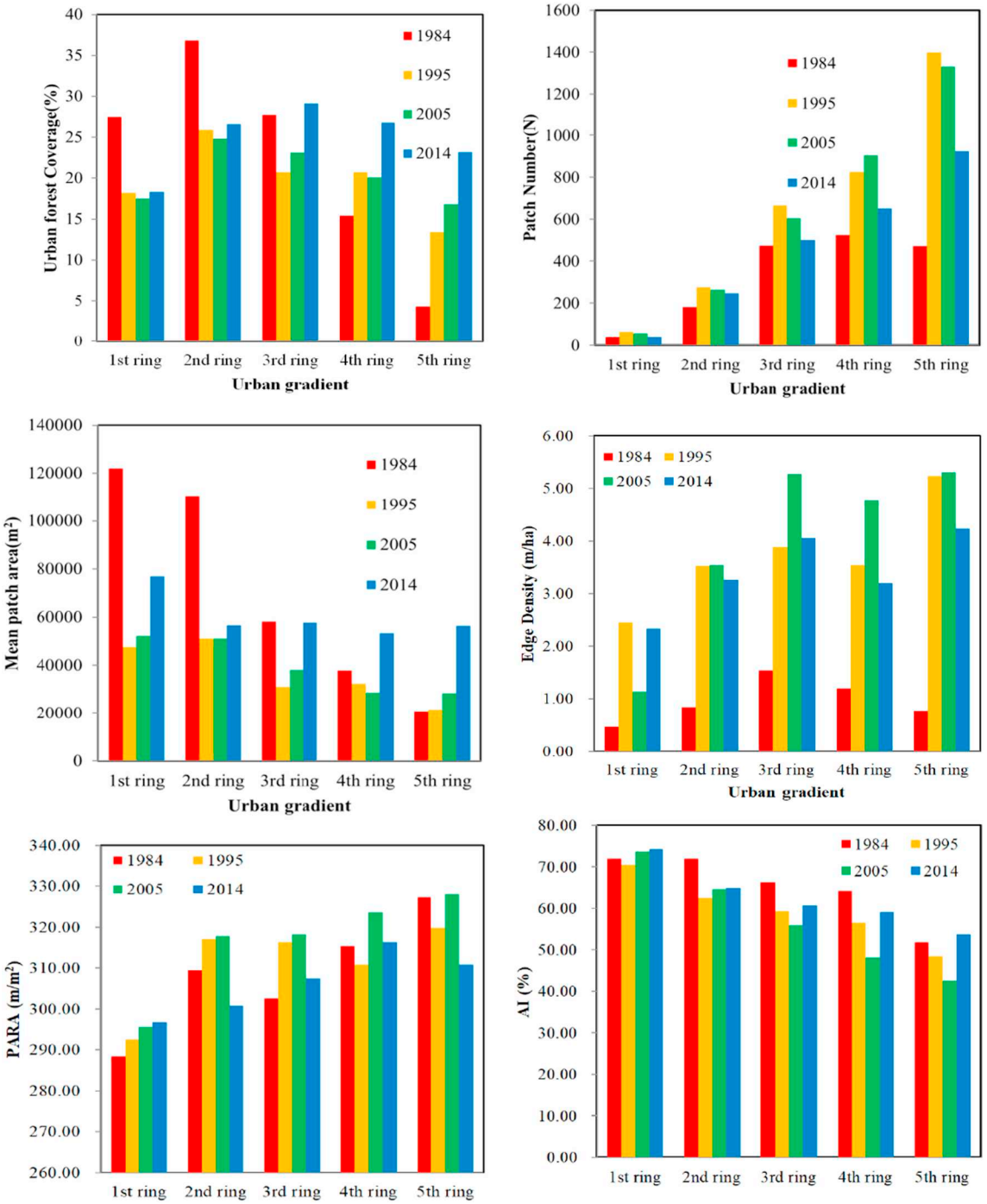

Fig. 6. Histograms showing temporal changes in UF coverage and landscape metrics across ring road-based urbanization gradient.

with the multitemporal TM images from 1984 to 2014, the selected best VI maps calculated from the multi-temporal TM images were then normalized to eliminate environmentally introduced radiometric effects. The relative radiometric correction method of pseudo-invariant feature (PIF) was applied in our study (Mitchell et al., 1997). This procedure uses one image as a reference image (2014) and then adjusts the radiometric properties of all other images (1984, 1995 and 2005) by the analysis of invariant features, such as roads, rooftops, and deep water. In our study, seventy-five spatial evenly distributed regions of interest for invariant features (including 25 from roads, 30 from rooftops, and 20 from water bodies) located on the multi-temporal images were manually selected. The average best VI in each selected region was then used to develop a linear normalization model between the reference image (2014) and the subject (i.e., uncorrected) images (1984, 1995 and 2005). Normalized subject images were obtained using the following equation:

$$VI_{ref} = a\,VI_{sub} + b$$

where VI_{ref} is the reference image (i.e., 2014 image); VI_{sub} is the subject image (i.e., 1984, 1995 and 2005 images), and a and b are linear regression coefficients.

A vector layer data of UF was first used to extract best VI of UF from

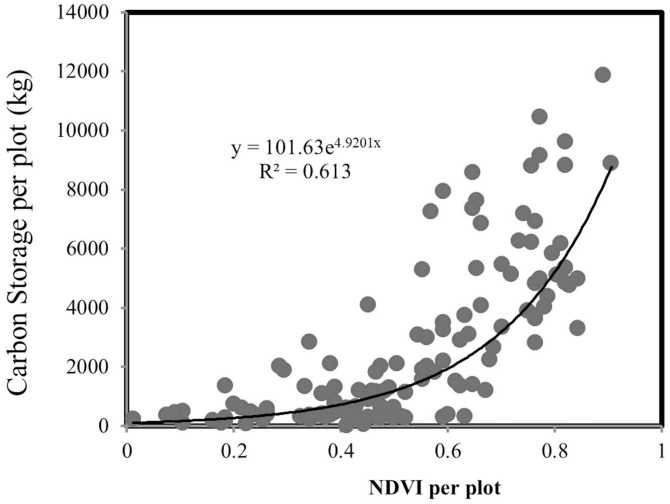

Fig. 7. Regression analyses of CS by UF vs. NDVI (n = 129, P < 0.01).

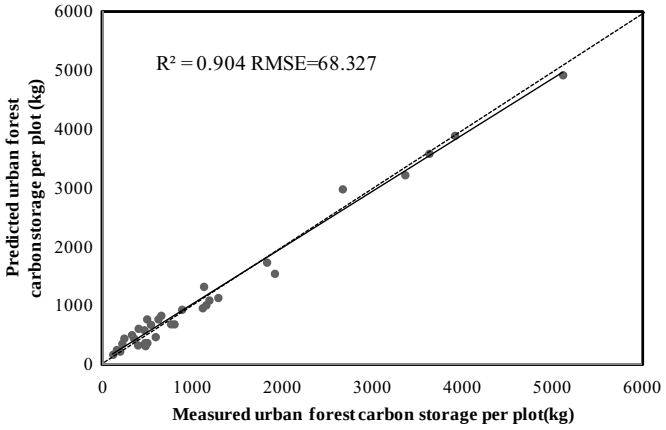

Fig. 8. Comparisons between plot-based measured CS by UF and the modeled CS by UF at the 30 sites (N = 30). Dotted line represents 1:1.

the 1984, 1995, 2005 and 2014 TM images. Then CS by UF map in 2014 was created by calculating pixel-based CS values using the regression model developed with the best VI extracted from 2014 VI image based on the 129 plot field survey data collected in 2013 and 2014. We also created spatio-temporal CS maps from normalized VI images calculated from the 1984, 1995 and 2005 TM images using the regression model of CS. Carbon density which is defined as UF carbon storage divided by UF area in a specific region was calculated at spatial and temporal scales.

2.6. Fossil fuel consumption and carbon emissions

We calculated the ratio of total CS by UF to the total carbon emissions from fossil fuel combustion in Changchun. The annual average carbon emissions from fossil fuel combustion in within the administrative boundary for Changchun for the years 1984, 1995, 2005, and 2014 were calculated based on published statistical data (Changchun Statistical Bureau, 1984, 1995, 2005, 2014). Consumption of different types of fossil fuels were first converted to equivalent consumption of standard coal based on the conversion coefficients (Supplementary Table 2), and then multiplied by 2.277 to convert to CO_2 (National Development and Reform Commission of China, 2007), and multiplied by 0.2727 (C percentage in CO_2:12/44) to convert to C.

3. Results

3.1. Spatio-temporal landscape patterns of UF in Changchun

Spatial distribution of UF in Changchun experienced dramatic changes over the past three decades. The coverage of UF steadily increased from 15% in 1984 to 25% in 2014 (Table 2). In 1984, UF was mostly distributed in downtown area, and then distributed more evenly with time across the whole urban area (Fig. 5). We found that UF became more fragmented from 1984 to 1995, and then it began to form a more homogeneous landscape since 1995. The value of UF patches density (PD) in 1995 was the greatest among the four study years. The total number of UF patches increased by approximately 99% from 1984 to1995, and then decreased by 2.6% from 1995 to 2005 and by 27.8% from 1995 to 2014 (Table 2). The values of mean UF patch size (PAM) showed a decrease of 43.4% from 1984 to 1995, and an increase of 14.9% from 1995 to 2005 and a doubling from 2005 to 2014. Edge density increased sharply from 1984 to 1995, while it decreased below 4.0 m/ha in 2014. Additionally, all other aggregation indices (AI, COHESION, LSI, etc.) indicated that UF of the city had the higher levels of aggregation in the years of 1984 and 2014.

The distribution of UF extended from downtown to outer suburban areas from 1984 to 2014. The coverage of UF increased gradually in outer suburban area (4th/5th-ring area), but decreased in the downtown area (1st/2nd-ring area) (Fig. 6). Patch numbers of UF showed an increasing trend from downtown area to outer suburban (Fig. 6). Furthermore, patch numbers of UF increased in all rings area from 1984 to 2005, especially in the 5th-ring area, but decreased from 2005 to 2014. Mean patch area of UF showed a decreasing trend from downtown to outer ring areas (Fig. 6). Meanwhile, mean patch area of UF increased gradually in outer suburban area (5th-ring), but decreased in downtown area (1st/2nd-ring area) of the city, especially in 2014. Edge density and PARA increased from downtown to outer ring area. The aggregation index AI decreased from downtown to outer ring area.

3.2. Spatio-temporal assessment model for CS

Five VIs were used as predictors for urban forest CS. The results show the urban forest CS were all significantly related to VIs except for NLI. The Pearson correlation coefficients between NDVI and urban CS were higher than between SR, GNDVI, NDMI and LAI (Table 1). This suggests that NDVI with higher correlation coefficients had stronger relationships with urban forest CS than other VIs. Therefore, NDVI was selected in our study to predict urban forest CS. It was shown that CS by UF had a positive non-linear relationship with NDVI (Fig. 7) and the non-linear model regression model with NDVI as independent variable explained 61.3% of total CS variance. CS by UF increased slowly with the increase of NDVI. When the value of NDVI was larger than 0.5, the CS increased sharply (Fig. 7). This model was then applied to produce the spatial distribution of CS from normalized historical NDVI images of 1984, 1995, and 2005. The results of validation showed that the value of modeled CS was very close the plot-measured CS (RMSE = 68.3 kg per plot; R^2 = 0.904) (Fig. 8). This indicated that the established model is reliable and can be used to predict CS by UF among the study years.

3.3. Spatio-temporal distribution of urban forest CS

In order to conduct spatiotemporal analyses of UF carbon storage with the multitemporal TM images from 1984 to 2014, the NDVI maps calculated from the multi-temporal TM images were normalized. Normalized subject images (Fig. 3) and the scene normalization coefficients of VI before and after normalization are listed in Table 2. By analyzing these pixel-based multi-year maps of CS by UF in ArcGIS platform, we found that CS in Changchun was highly dynamic in the four study years (Figs. 9, 10). Due to the expansion of UF distribution, CS for Changchun increased gradually during the whole period with the

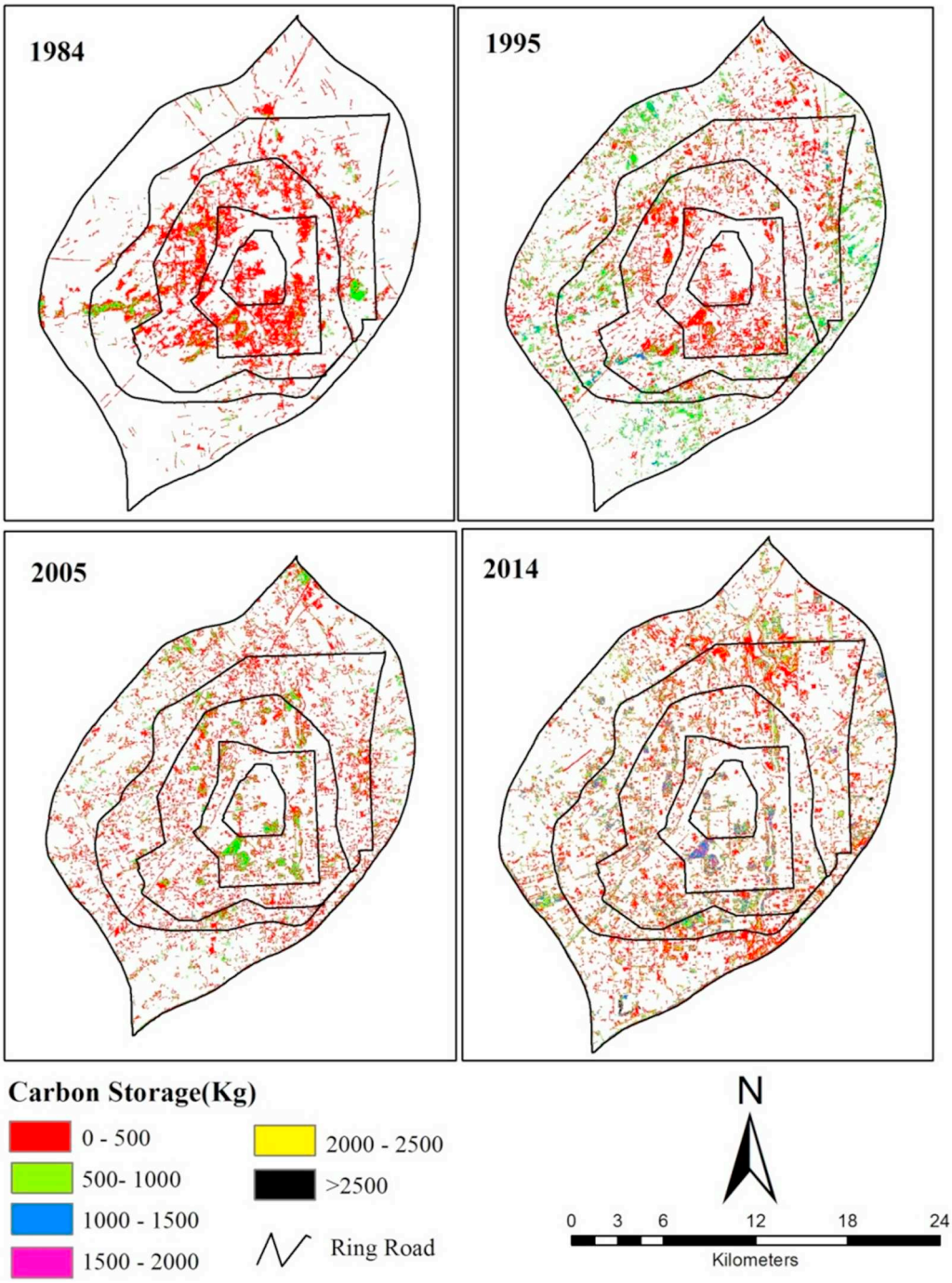

Fig. 9. Spatio-temporal distribution of CS by UF based on pixels in the City of Changchun.

values of 68 Gg in 1984, 129 Gg in 1995, 167 Gg in 2005 and 224 Gg t in 2014, respectively. In addition, the high spatial variation of CS was observed across the city. With urban expansion, an obvious change of CS by UF first occurred in the urban fringe and suburban area (Fig. 11). In 1984, pixels with high values of CS were mostly concentrated in downtown areas (Figs. 9, 10) and were distributed more evenly across the whole urban area in recent years (2005 and 2014). There was also a decreasing trend from outer suburban areas to downtown areas in the years 1995, 2005 and 2014 (Fig. 10).

Meanwhile, UF carbon density was higher within 2nd ring than within other rings of the city for the years of 1984, 1995, 2005 and 2014 (Fig. 10). Our results also showed that the different spatial changes of CS by UF have occurred across different urbanization gradients from 1984 to 2014. It is obvious that total CS by UF increased more in the outer suburban area than in downtown area (Fig. 10). However, UF carbon density had greater increase in downtown area than that in the outer suburban area of the city.

The distribution of UF patches were all skewed toward low carbon storage values all in the years. The CS by UF class of 0–500 kg per pixel had the highest frequency with the value of 66%, 53%, 55% and 40% in 1984, 1995, 2005 and 2014, respectively (Fig. 12). We found that the frequency of lower CS by UF (< 500 kg) decreased gradually from 1984, 1995, 2005 to 2014. Meanwhile, the frequency of higher CS by UF (> 1500 kg) increased gradually from 4% in 1995 to 11% in 2005.

About 7% of CS by UF was in the class above 2000 kg in 2014, but with just a few pixels with CS > 2000 kg in 1984, 1995 and 2005.

4. Discussion

4.1. Spatio-temporal changes of UF under China's rapid urban expansion and urban greening

In this study, we found that UF coverage in Changchun was gradually increased over time (Table 2 and Figs. 5, 6). The changing patterns of UF in the metropolitan area dramatically responded to the combined effects of rapid urban expansion and urban greening policies (Fig. 4). Previous studies showed that UF in China developed rapidly, especially in suburban areas with the accelerating urban sprawl (Zhou and Wang, 2011; Tian et al., 2005). Distinct increases of UF area were also observed in the present study from 1984 to 2014. This phenomenon was opposite to the trend of UF change in most Eastern European cities and cities in the USA (Dallimer et al., 2011; Baycanlevent et al., 2009; Kabisch and Haase, 2013; Nowak and Greenfield, 2012). To some extent, the opposite trend could be attributed to different urban development patterns in different countries. There are two main urban development patterns in the world (Dallimer et al., 2011); city sprawl into the wider countryside and increase in density through the development of current urban area. In Europe and USA, some cities developed through densifying the current urban area, which could result in UF decline. In contrast, most cities in China have expanded by extending “sprawl” into the wider countryside where more new UF was established. Local governments realize that UF has an important environmental function and have established a series of greening policies. The State Forestry Administration of the People's Republic of China facilitated a plan called “Constructing Forest cities”. This program pushes local governments to invest a large amount of money to introduce green elements into urban areas to resolve urban environmental problems (Jiang and Zhang, 2010; Wang, 2016). In addition, more and more new UF parks and community gardens have been established, especially for national UF parks in suburban areas. In our study, we noticed that the urban greening policy has stimulated the dramatic increase of UF area in Changchun from 1984 to 1995. Although total UF area increased with the development of urbanization and urban greening, UF in the central urban area became more and more fragmented due to intense urbanization from 1984 to 1995. Along with rapid urban greening since 1995, UF patches became larger and larger when compared with the spatial patterns in 1995. In spite of the increasing UF amount, some planning strategies are still needed. Conservation or construction plans in the urban core areas are required to protect UF from potential loss caused by urbanization, particularly within the 1st-ring road where built-up land has increased (Zhao et al., 2010). The results of our study also showed that the distribution of UF is uneven in Changchun with higher UF cover in suburban areas than in urban core areas, especially those within the 1st ring. Therefore, urban planners and policy makers should be concerned with the distribution inequity of UF and plant more suitable trees to increase the amount of UF in urban central areas.

4.2. The spatio-temporal estimation of urban CS in Changchun

Our results showed that CS by UF could be estimated by NDVI extracted from TM imagery similar to successful estimation of natural forest CS or biomass by NDVI (Lu et al., 2004; Ingram et al., 2005). However, our studies showed that the relationship between forest CS and NDVI was weaker in urban areas than that in natural areas (Simone et al., 2005; Hall et al., 2006). One possible reason might be that the environment in urban area is complex and the structure and composition of UF is very different from that of natural forests. Usually, the heterogeneous and fragmented landscape in cities may result in a mixed pixel problem which might be one of the main reasons for the poor

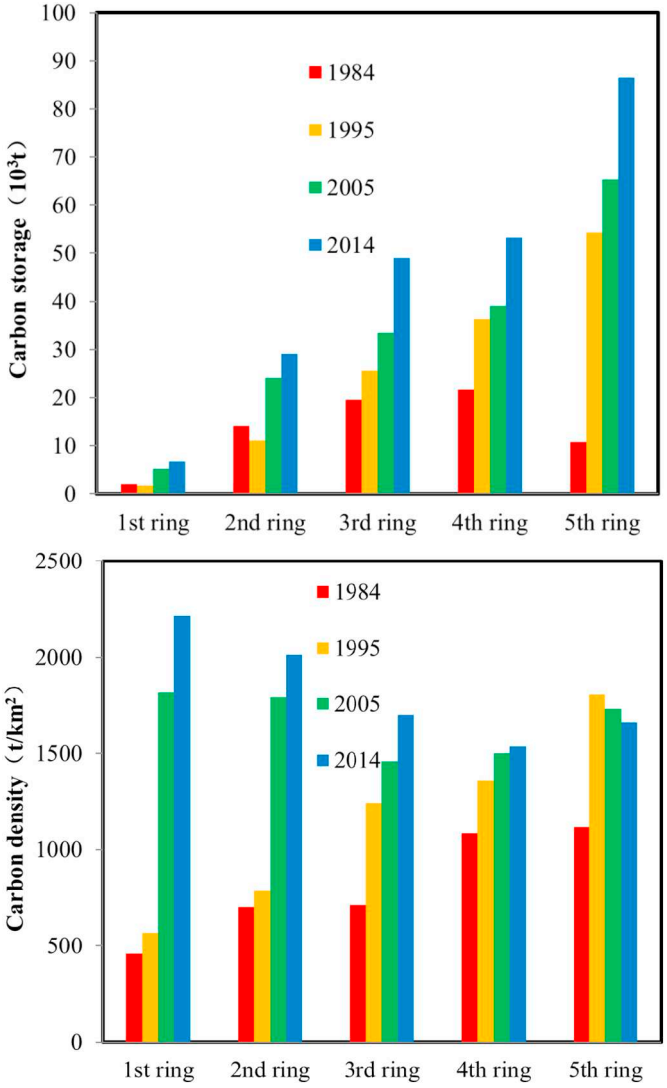

Fig. 10. CS by UF and carbon density based on pixels across urbanization gradient.

success of urban vegetation carbon storage by NDVI. In the present study, we selected UF rather than urban green space or green land which diminished the mixed pixel problem. The approach of establishing a model to predict CS by UF has been relatively successful, but it still has some limitations. The major limitation of using vegetation indices (VIs) to estimate forest CS is that VIs frequently lose sensitivity and saturate at moderately high biomass or leaf area index (LAI) (e.g., Baret and Guyot, 1991; Gower et al., 1999; Gray and Song, 2012). The nonlinear equations between NDVI and CS by UF or biomass and the existence of a saturation effect of NDVI in UF found in this study and similar to natural forest also verified this limitation. However, such a limitation was of lesser importance in and urban setting since CS by UF from most urban vegetated areas in this study were much lower than that in natural forest area and few of the UF had canopy density above 60% (Hall et al., 2006; Gray and Song, 2012).

In this study, we found that the spatial distribution of CS by UF was very dynamic, mirroring the intense urbanization and rapid development of urban greening in the city. The carbon storage of UF was also found to vary across the different urbanization gradients (Fig. 10). CS by UF decreased from suburban areas to downtown areas for all study years. It moves in the opposite direction to the increasing urbanization intensity from suburban areas to downtown areas in China (Zhou and

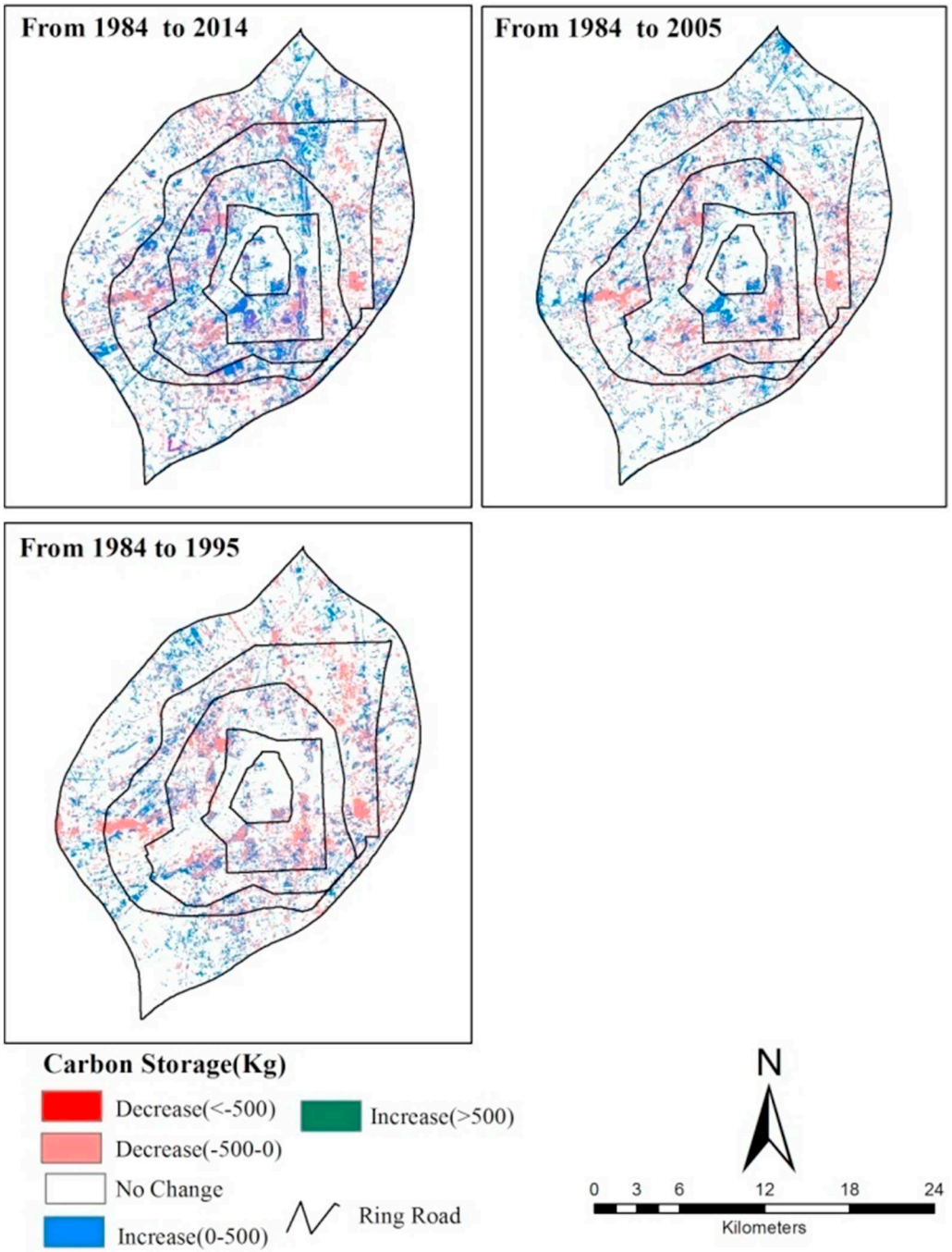

Fig. 11. Spatio-temporal changing patterns of CS by UF based on pixels in the City of Changchun.

Wang, 2011). The changing patterns of CS by UF in the metropolitan area of Changchun, China from 1984 to 2014 responded to combined effects of rapid urbanization and greening policies (Fig. 4). The UF carbon density in Changchun was 1.68 kg/m^2, 1.59 kg/m^2, 1.45 kg/m^2, 0.87 kg/m^2 for the years of 1984, 1995, 2005, and 2014, respectively. This carbon density value was lower than Seattle, WA (8.98 kg/m^2) and Sacramento, CA (4.69 kg/m^2), both in USA (McPherson et al., 2013), and cities in China like Beijing (4.37 kg/m^2) (Yang et al., 2005), Xiamen (2.08 kg/m^2) (Ren et al., 2012), and Hangzhou (3.03 kg/m^2) (Zhao et al., 2010). The reason is that UF in Changchun is mostly made up of young trees due to the recent fast urbanization and greening mentioned previously (Zhang et al., 2015). This also implies that UF in Changchun has great potential for CO_2 assimilation in the future. In addition, since UF in the present study was defined as "urban green space patches of at least 0.5 ha in size", numerous green space patches < 0.5 ha were excluded. This may be a major reason for the large difference between UF coverage (25%) found in our study and urban vegetation coverage (45%) reported by the municipal government. By excluding green patches < 0.5 ha, CS by above-ground biomass of urban plants was also underestimated in the city.

The ratio of total annual C sequestration by UF to urban CO_2 emission from energy consumption was within the broad range of 0.2% in Beijing (Yang et al., 2005) and 18.57% in Hangzhou (Zhao et al., 2010). It should be noted that in Changchun, when calculating the amounts of carbon stored and sequestered by UF, we only considered the UF within the 5th-ring road area, but C emissions reported by

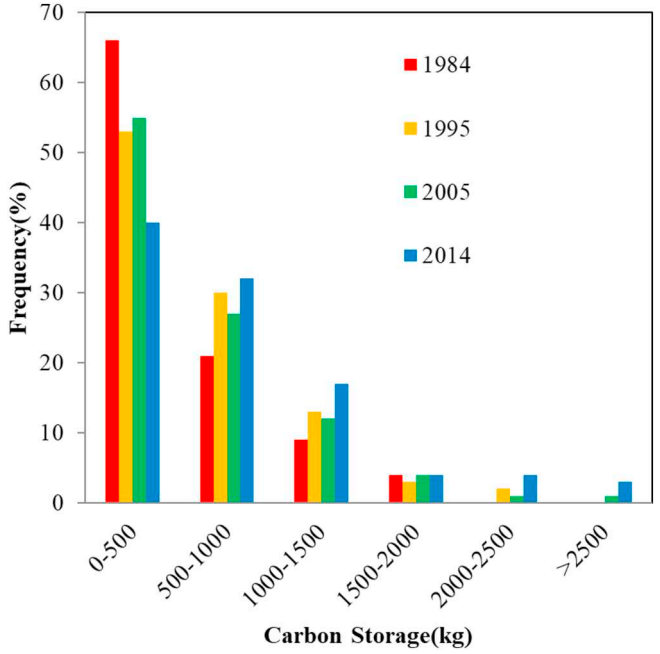

Fig. 12. Histograms of the frequency statistics for CS by UF, calculated from pixels with UF in the study area of Changchun.

Changchun Statistical Bureau were for the entire Changchun area extending on average 60 km beyond the 5th ring road. The area of C emissions reported by the Changchun Statistical Bureau is definitely much larger than that of the UF in our study. Consequently, the mitigation of urban CO_2 emission by the UF was underestimated. Meanwhile, our results also showed that most areas in Changchun still had low CS or biomass values. These results suggest that there is great potential to increase the capacity of CS by UF and mitigate CO_2 emission. The above results have some important management implications for climate mitigation from urban greening. There is still great potential to increase the total area of UF in Changchun from its current cover of only 25%. More trees can be planted especially in suburban areas and more carbon can be sequestered. We should seek practical approaches to optimize UF structure to enhance the capacity of UF in CS and sequestration. Some practical measures are suggested such as selecting appropriate tree species, and improving spatial distribution, pruning and shaping. Native species such as poplar and willow with fast growth rates should be planted to improve the capacity of CS and sequestration; multilayer forest communities with high canopy density and LAI are the most effective.

The present study provides baseline information at landscape level by producing relatively high-resolution maps of UF and its CS. The spatio-temporal information of UF and its CS may provide urban planners with information to conduct more realistic and better planting designs of UF at an urban landscape level. With urban sprawl, UF increases rapidly, and could serve as an important C stock in cities. CS by UF in Changchun increased from 68 Gg in 1984 to 224 Gg in 2014, with an annual increment of 5.2 Gg. Our study also showed that the annual average increase of C emissions from combustion of fossil fuels in Changchun was 195.8 Gg (1213 Gg, 3336 Gg, 5616 Gg, 7087 Gg for the years of 1984, 1995, 2005, and 2014) (Table 3). We can conclude that roughly 3.9% of the annual increase of C emissions could be offset by the annual increase of CS by UF. CS by UF was equal to 5.60%, 3.87%, 2.97%, and 3.16% of the annual average C emissions for the years of 1984, 1995, 2005 and 2014, respectively.

In addition, there are also some limitations for our study. Our results showed that VI derived models can be used to predict CS by UF across cities from TM imagery. However, it should be noted that the different climatic conditions, such as precipitation and temperature in different cities may significantly influence the relationship between VI and CS by UF (Schmidt et al., 2014). Whether the relationship between them changes across different climatic region is also still unknown. In addition, TM imagery can mainly be used to detect the uppercrown surface of forests in a two-dimensional pace. Light Detection And Ranging (LiDAR) imagery in recent years can provide fine-scale three dimensional structure of forest, which would be of great importance for mapping of CS in urban landscape with high accuracy (Mitchell et al., 2018). We just conducted studied for one city in one climatic zone type, more comparative research for different cities should be considered to explore the relationship between urbanization and urban CS by UF.

5. Conclusion

This study demonstrated the potential of using historical Landsat TM imagery combined with urban forest (UF) field survey data to estimate spatio-temporal patterns of UF and its carbon storage (CS) in in the City of Changchun, China. We found that NDVI is a good predictor to estimate and map CS by UF. Landsat TM can provide a fast and cost-effective method to obtain spatio-temporal patterns of 30-m resolution CS by UF. Quantifying the spatio-temporal function of CS by UF may help the decision-makers and the public better understand the role of UF in reducing atmospheric CO_2.The UF and its CS in Changchun increased significantly and continuously from 1984, 1995, 2005 and to 2014, especially in the outer suburban areas of the city due to urban sprawl. The CS by UF class distribution was skewed toward low values in all the years, but the skew gradually decreased over time. The final spatio-temporal patterns of CS by UF from TM images would have important implications for CO_2 mitigation under China's rapid urbanization and urban greening and could provide more information about how to establish UF to maximize its ecological benefit of CO_2 mitigation, particularly for cities where UF is still under construction.

Table 3
Summary of UF attributes within the study area in the City of Changchun.

Year	TA (ha)	Coverage (%)	NP (n)	PD (n/10^{2}ha)	PAM (ha)	ED (m/ha)	LPI (%)	LSI (—)	AI (%)	Cohesion (%)
2014	13,356	25	2174	16.25	6.13	3.92	4.94	34.93	56.20	80.96
2005	10,480	20	2934	27.99	3.57	4.93	3.22	53.78	48.18	69.66
1995	8908	17	3031	33.82	2.96	4.24	3.04	56.53	52.76	73.54
1984	7856	15	1014	12.9	7.75	1.21	22.81	56.27	64.74	94.13

Notes: TA: Total Area; NP: Number of Patches; PD: Patch Density; PAM: Patch Area Mean; ED: Edge Density; LPI: Largest Patch Index; LSI: Landscape Shape Index; AI: Aggregation Index; COHESION: Patch Cohesion Index.

Acknowledgments

This research was supported by Foundation for Excellent Young Scholars of Northeast Institute of Geography and Agroecology, Chinese Academy of Sciences (DLSYQ13004), the National Natural Science Foundation of China (41701210), Science Development Project of Jilin Province, China (20180418138FG), and "Strategic Planning Project from Institute of Northeast Geography and Agroecology (IGA), Chinese Academy of Sciences" (Y6H2091001), the National Natural Science Foundation of China (Grant No. 41601094). The authors express gratitude to the editors and the anonymous reviewers who gave us their insightful comments and suggestions.

Appendix A. Supplementary data

Supplementary data to this article can be found online at https://doi.org/10.1016/j.envint.2019.05.010.

References

Baret, F., Guyot, G., 1991. Potentials and limits of vegetation indices for LAI and APAR assessment. Remote Sens. Environ. 35, 161–173.
Baycanlevent, T., Vreeker, R., Nijkamp, P., 2009. A multi-criteria evaluation of green spaces in European cities. Eur Urban Reg Stud 16, 193–213.
Chander, G., Markham, B., 2003. Revised Landsat-5 TM radiometric calibration procedures and postcalibration dynamic ranges. IEEE Trans Geosci Remote Sensing 41, 2674–2677.
Cohen, W.B., Spies, T.A., Fiorella, M., 1995. Estimating the age and structure of forests in a multi-ownership landscape of western Oregon, U.S.A. Int. J. Remote Sens. 16, 721–746.
Dallimer, M., Tang, Z.Y., Bibby, P.R., Brindley, P., Gaston, K.J., Davies, Z.G., 2011. Temporal changes in greenspace in a highly urbanized region. Biol. Lett. 7, 763.
Escobedo, F., Varela, S., Zhao, M., Wagner, J.E., Zipperer, W., 2010. Analyzing the efficacy of subtropical urban forests in offsetting carbon emissions from cities. Environ. Sci. Pol. 13, 362–372.
Frolking, S., Palace, M.W., Clark, D.B., Chambers, J.Q., Shugart, H.H., Hurtt, G.C., 2009. Forest disturbance and recovery: a general review in the context of spaceborne remote sensing of impacts on aboveground biomass and canopy structure. J Geophys Res-Biogeosci 114, 281–296.
Gao, Y., Mas, J.F., 2008. A comparison of the performance of pixel based and object based classifications over images with various spatial resolutions. Online J Earth Sci 1, 27–35.
Gaston, K.J., Ávila-Jiménez, M.L., Edmondson, J.L., Jones, J., 2013. Review: managing urban ecosystems for goods and services. J. Appl. Ecol. 50, 830–840.
Gower, S.T., Kucharik, C.J., Norman, J.M., 1999. Direct and indirect estimation of leaf area index, f APAR, and net primary production of terrestrial ecosystems. Remote Sens. Environ. 70, 29–51.
Gray, J., Song, C.H., 2012. Mapping leaf area index using spatial, spectral, and temporal information from multiple sensors. Remote Sens. Environ. 119, 173–183.
Hall, R.J., Skakun, R.S., Arsenault, E.J., Case, B.S., 2006. Modeling forest stand structure attributes using Landsat ETM+ data: application to mapping of aboveground biomass and stand volume. For. Ecol. Manag. 225, 378–390.
Heath, L.S., Smith, J.E., Skog, K.E., Nowak, D.J., Woodall, C.W., 2011. Managed Forest carbon estimates for the US greenhouse gas inventory, 1990–2008. J. For. 109, 167–173.
Ingram, J.C., Dawson, T.P., Whittaker, R.J., 2005. Mapping tropical forest structure in southeastern Madagascar using remote sensing and artificial neural networks. Remote Sens. Environ. 94, 491–507.
Ji, L., Wylie, B.K., Nossov, D.R., Peterson, B., 2012. Estimating aboveground biomass in interior Alaska with Landsat data and field measurements. Int. J. Appl. Earth Obs. Geoinf. 18, 451–461.
Jiang, Y.X., Zhang, W.Y., 2010. On Forest City and low-carbon city. J Chin Urban For 8, 4–7 (In Chinese).
Kabisch, N., Haase, D., 2013. Green spaces of European cities revisited for 1990–2006. Landsc. Urban Plan. 110, 113–122.
Kayitakire, F., Hamel, C., Defourny, P., 2006. Retrieving forest structure variables based on image texture analysis and IKONOS-2 imagery. Remote Sens. Environ. 102, 390–401.
Kwok, A., Cheung, L., Brierley, G., Sullivan, D.O., 2016. Landscape structure and dynamics on the Qinghai-Tibetan Plateau. Ecol. Model. 339, 7–22.
Lee, J.H., Ko, Y., McPherson, E.G., 2016. The feasibility of remotely sensed data to estimate urban tree dimensions and biomass. Urban For & Urban Green 16, 208–220.
Liu, C.F., Li, H.M., He, X.Y., Chen, W., Xu, W.D., Zhao, G.L., Ning, Z.H., 2003. Concept discussion and analysis of urban forest. Chin J Ecol 22, 146–149 (in Chinese).
Liu, C.F., Li, X.M., 2012. Carbon storage and sequestration by urban forests in Shenyang, China. Urban For. Urban Green. 11, 121–128.
Lu, D.S., Mausel, P., BrondíZio, E., Moran, E., 2004. Relationships between forest stand parameters and Landsat TM spectral responses in the Brazilian Amazon Basin. For. Ecol. Manag. 198, 149–167.
Lucy, R.H., Byungman, Y., Marina, A., 2010. Terrestrial carbon stocks across a gradient of urbanization:a study of the Seattle, WA region. Glob. Chang. Biol. 17, 783–797.
Lv, H., Wang, W., He, X., 2016. Quantifying tree and soil carbon stocks in a temperate urban forest in Northeast China. Forests 7 (9), 1–13.
McGarigal, K., Cushman, S., Ene, E., 2012. FRAGSTATS v4: spatial pattern analysis program for categorical and continuous maps. http://www.umass.edu/landeco/research/fragstats/fragstats.html.
McPherson, E.G., Xiao, Q.F., Aguaron, E., 2013. A new approach to quantify and map carbon stored, sequestered and emissions avoided by urban forests. Landsc. Urban Plan. 120, 70–84.
Mitchell, R.M., O'Brien, D.M., Edwards, M., Graetz, R.D., 1997. Selection and initial characterization of a bright calibration site in the Strzelecki Desert, South Australia. Can. J. Remote. Sens. 23, 342–353.
Mitchell, M.G.E., Johansen, K., Maron, M., McAlpine, C.A., Wu, D., Rhodes, J.R., 2018. Identification of fine scale and landscape scale drivers of urban aboveground carbon stocks using high-resolution modeling and mapping. Sci. Total Environ. 622–623, 57–70.
Narine, L.L., Popescu, S., Neuenschwander, A., 2019. Estimating aboveground biomass and forest canopy cover with simulated ICESat-2 data. Remote Sens. Environ. 224, 1–11.
National Development and Reform Commission of China, National, 2007. China's National Climate Change Programme. Retrieved January 15th, 2009 from. http://www.chinaembassy.org.sg/chn/xwdt/P020070611577558281561.pdf.
Nero, B., Callo-Concha, D., Denich, M., 2018. Diversity, and carbon stocks of the tree community of Kumasi, Ghana. Forests. 9 (9), 1–10.
Nowak, D.J., 1994. Understanding the structure of urban forests. J. For. 92, 42–46.
Nowak, D.J., Crane, D.E., 2002. Carbon storage and sequestration by urban trees in the USA. Environ. Pollut. 116, 381–393.
Nowak, D.J., Greenfield, E.J., 2012. Tree and impervious cover in the United States. Landsc. Urban Plan. 107, 21–30.
Nowak, D.J., Crane, D.E., Stevens, J.C., Hoehn, R.E., 2003. The Urban Forest Effects (UFORE) Model: Field Data Collection Manual. USDA Forest Service, Syracuse, NY.
Nowak, D.J., Greenfield, E.J., Hoehn, R.E., Lapoint, E., 2013. Carbon storage and sequestration by trees in urban and community areas of the United States. Environ. Pollut. 178, 229–240.
Pei, N., Wang, C., Jin, Ji, 2018. Long-term afforestation efforts increase bird species diversity in Beijing, China. Urban For & Urban Green 29, 88–95.
Raciti, S.M., Hutyra, L.R., Newell, J.D., 2014. Mapping carbon storage in urban trees with multi-source remote sensing data: relationships between biomass, land use, and demographics in Boston neighborhoods. Sci. Total Environ. 500–501, 72–83.
Rao, P., Hutyra, L.R., Raciti, S.M., Finzi, A.C., 2013. Field and remotely sensed measures of soil and vegetation carbon and nitrogen across an urbanization gradient in the Boston metropolitan area. Urban Ecosyst 16, 593–616.
Ren, Y., et al., 2012. Effects of rapid urban sprawl on urban forest carbon stocks: integrating remotely sensed, GIS and forest inventory data. J. Environ. Manag. 113, 447–455.
Roy, P.S., Ranganath, B.K., Diwakar, P.G., Vohra, T.P.S., Bhan, S.K., Singh, I.J., Pandian, V.C., 1991. Tropical forest typo mapping and monitoring using remote sensing. Int. J. Remote Sens. 12, 2205–2225.
Schindler, S., Wehrden, H.V., Poirazidis, K., Hochachka, W.M., Wrbka, T., Kati, V., 2015. Performance of methods to select landscape metrics for modeling species richness. Ecol. Model. 295, 107–112.
Schmidt, M., Klein, D., Conrad, C., Dech, S., Paeth, H., 2014. On the relationshipbetween vegetation and climate in tropical and northern Africa. Theor. Appl. Climatol. 115, 341–353.
SFA, 2018. 3-19. Available online. http://www.forestry.gov.cn/main/72/content-1083701.html.
Simone, R.F., Marcia, C.S., Carla, B.M., 2005. Relationships between forest structure and vegetation indices in Atlantic Rainforest. For. Ecol. Manag. 218, 353–362.
Strohbach, M.W., Haase, D., 2011. Above-ground carbon storage by urban trees in Leipzig, Germany: analysis of patterns in a European city. Landsc. Urban Plan. 104, 95–104.
Sun, Y., Xie, S., Zhao, S., 2019. Valuing urban green spaces in mitigating climate change: a city-wide estimate of aboveground carbon stored in urban green spaces of China's capital. Glob. Chang. Biol. 25 (5), 1717–1732.
Tian, G.J., Liu, J.Y., Xie, Y.C., Yang, Z.F., Zhuang, D.F., Niu, Z., 2005. Analysis of spatio-temporal dynamic pattern and driving forces of urban land in China in 1990s using TM images and GIS. Cities 22, 400–410.
Wang, C.K., 2006. Biomass allometric equations for 10 co-occurring tree species in Chinese temperate forests. For. Ecol. Manag. 222, 9–16.
Wang, C., 2016. Some issues of forest city cluster construction in China. J Chin Urban For 14, 1–6 (in Chinese).
Wang, W., Zhang, B., Zhou, W., 2019. The effect of urbanization gradients and forest types on microclimatic regulation by trees, in association with climate, tree sizes and species compositions in Harbin city, northeastern China. Urban Ecosyst 22, 367–384.
Wu, F., Wu, Z.M., Wu, W.Y., 2012. Appraisal of carbon storage in urban forest patches and its distribution pattern in Maanshan city. J Anhui Agric Univ 39, 519–526 (in Chinese).
Yang, J., Mcbride, J., Zhou, J.X., Sun, Z.Y., 2005. The urban forest in Beijing and its role

in air pollution reduction. Urban For. Urban Green. 3, 65–78.
Yang, J., Huang, C.H., Zhang, Z.Y., Wang, L., 2014. The temporal trend of urban green coverage in major Chinese cities between 1990 and 2010. Urban For. Urban Green. 13, 19–27.
Zhang, D., et al., 2015. Effects of forest type and urbanization on carbon storage of urban forests in Changchun, Northeast China. Chin. Geogr. Sci. 25, 147–158.
Zhao, M., Kong, Z.H., Escobedo, F.J., Gao, J., 2010. Impacts of urban forests on offsetting carbon emissions from industrial energy use in Hangzhou, China. J. Environ. Manag. 91, 807–813.
Zhao, J.J., Chen, S.B., Jiang, B., Ren, Y., Wang, H., Vause, J., Yu, H.D., 2013. Temporal trend of green space coverage in China and its relationship with urbanization over the last two decades. Sci. Total Environ. 442, 455–465.
Zhou, W.Q., Troy, A., 2009. Development of an object-based framework for classifying and inventorying human-dominated forest ecosystems. Int. J. Remote Sens. 30, 6343–6360.
Zhou, X.L., Wang, Y.C., 2011. Spatial-temporal dynamics of urban green space in response to rapid urbanization and greening policies. Landsc. Urban Plan. 100, 268–277.